Polymer Bulletin (2020) 77:4077–4094
https://doi.org/10.1007/s00289-019-02955-0

ORIGINAL PAPER

High optical transparency, low dielectric constant and light color of organosoluble fluorinated polyimides based on 10,10-bis[4-(4-amino-3-trifluoromethylphenoxy) phenyl]-9(*10H*)-anthrone

Ting Zhang[1] · Yang Pan[1] · Cheng Song[1] · Bin Huang[1] · Zhen-Zhong Huang[1]

Received: 20 June 2019 / Revised: 3 September 2019 / Accepted: 10 September 2019 /
Published online: 14 September 2019

Abstract

A new aromatic diamine bearing ether, trifluoromethyl and anthrone groups, 10,10-bis[4-(4-amino-3-trifluoromethylphenoxy)phenyl]-9(*10H*)-anthrone (BATFPA) was prepared in three steps from anthrone. BATFPA was reacted with six conventional aromatic dianhydrides in *N*,*N*-dimethylacetamide (DMAc) to form the corresponding cardo fluorinated polyimides (PIs) via the poly(amic acid) (PAA) precursors with inherent viscosities ranging from 0.82 to 1.18 dL/g and thermal imidization. All the PAAs could be cast from DMAc solution and thermally converted into transparent, flexible and tough PI films with tensile strength of 63.5–101.7 MPa, tensile modulus of 1.94–2.85 GPa and elongation at break of 3.7–13.6%. The resulting PIs were predominantly amorphous and exhibited good solubility in dipolar solvents such as DMAc, *N,N*-dimethylformamide and *N*-methyl-2-pyrrolidinone at room temperature. In particular, the PI derived from 4,4′-hexafluoroisopropylidenediphthalic anhydride was even soluble in tetrahydrofuran. These new PIs displayed excellent thermal stability with T_g of 259–329 °C, 5% weight loss temperature (T_{d5}) of 516–530 °C and the residue of 57–64% at 800 °C in nitrogen. Meanwhile, these PIs also had low moisture absorptions (0.36–0.83%), low dielectric constants (2.35–2.96 at 1 MHz), good optical transparency with cutoff wavelengths of ultraviolet–visible absorption at 336–408 nm and more than 80% transmittance at 600 nm.

Keywords Fluorinated polyimides · Cardo anthrone pendent unit · Trifluoromethyl group

✉ Yang Pan
panyang@jxnu.edu.cn

✉ Zhen-Zhong Huang
huangzz@jxnu.edu.cn

[1] Key Laboratory of Functional Small Organic Molecule of Ministry of Education, Jiangxi Normal University, Nanchang 330022, China

Introduction

In recent years, heat-resistant optically transparent polymers are extensively investigated for their particular potential applications in electronic and optoelectronic fields owing to their several distinct advantages such as lightness, flexibility and good processability [1–3]. Ideal polymers with critical features including high heat resistance, excellent optical transparency, essential colorlessness, outstanding mechanical properties, solution processability and good dimensional stability are expected to meet the requirement. Obviously, traditional thermoplastic engineering plastics [4], such as polycarbonate ($T_g = 145$ °C) and poly(ether sulfone) ($T_g = 225$ °C), do not fulfill the requirement for high-temperature manufacturing in electronics industry owing to their low T_g's, where long-term service temperature of 270 °C (for lead-free solder reflowing) and short-term service temperature of 400 °C (for silicon-based TFT fabrication) are required. Therefore, development of highly optical transparent polymers with high heat resistance is still an urgent need, which attracts more and more attention of researchers from both academic and commercial perspectives. Aromatic polyimides (PIs) have been used in the electronic, automotive and aerospace industries due to their extremely high T_g, good thermal stability and chemical resistance, excellent mechanical and electrical properties [5–8]. However, the intensive coloration of the PIs, owing to electronic conjugation and the formation of inter- and intramolecular charge transfer complexes (CTC), limits their applications in optical and optoelectronic fields. Therefore, many efforts have been made to obtain highly transparent PIs through various strategies, including introduction of bulky substituents [9–13], alicyclic units [14–16], asymmetry and non-coplanar structures [17–19] into the polymer backbones. These structural modifications could loosen the chain packing, disrupt the conjugation and inhibit the formation of CTC, leading to colorless PIs. Among them, it was found that incorporation of the fluorine groups like trifluoromethyl group into the PI backbones resulted in great benefits for improving the polymers' properties such as solubility and optical transparency, as well as reducing their moisture absorption, crystallinity, dielectric constant and color, which is attributed to the small dipole and the low polarizability of the C–F band as well as the increase in free volume [20–25]. Furthermore, introduction of bulky loops substituents (usually named as cardo groups) (e.g., cyclododecane, adamantine, fluorine, phthalide and xanthene) into the PI main chains not only inhibits the close packing of polymer chains to improve their solubility without sacrificing the thermal stability, but also reduces the CTC formation to yield transparent and colorless films [26–32]. The cardo anthrone group has been incorporated into the polymer backbones such as polyamides and polyimides derived from 10,10-bis(4-aminophenyl)-9(*10H*)-anthrone, as well as polyarylates and poly(1,3,4-oxadiazole)s based on 10,10-bis(4-carboxyphenyl)-9(*10H*)-anthrone to improve the processability [26]. However, to our knowledge, no work has been done on the fluorinated PIs bearing both a flexible ether linkage and a bulky anthrone pendent group in the polymer backbones. In view of the mentioned reasons as above, introducing ether, trifluoromethyl and

anthrone groups into the molecular skeletons simultaneously might generate new soluble high-temperature PIs with excellent combined properties. In the present study, a new aromatic diamine composed of ether, trifluoromethyl and anthrone units, 10,10-bis[4-(4-amino-3-trifluoromethylphenoxy)phenyl]-9(*10H*)-anthrone (**BATFPA**) was synthesized, and a series of fluorinated PIs were prepared from **BATFPA** and various commercial aromatic dianhydrides by a conventional two-step procedure. The general properties such as solubility, crystallinity, optical, dielectric, thermal and mechanical properties of the resulting cardo PIs were investigated. The effect of the functional groups like anthrone pendent group on their properties such as solubility and crystallinity is also discussed in this paper.

Experimental

Materials

Commercially available chemicals (Shanghai Chemical Reagents Corp., China) such as 9(*10H*)-anthrone, phenol, thionyl chloride 2-chloro-5-nitrotrifluoromethylbenzene, hydrazine monohydrate, potassium carbonate, and 10% palladium on activated carbon were used without further purification. Pyromellitic dianhydride (PMDA, **4a**), 3,3′,4,4′-biphenyltetracarboxylic dianhydride (BPDA, **4b**), 1,4-bis(3,4-dicarboxyphenoxy)benzene dianhydride (HQDPA, **4c**), 3,3′,4,4′-benzophenonetetracarboxylic dianhydride (BTDA, **4d**), 2,2′-bis(3,4-dicarboxyphenyl)hexafluoropropane dianhydride (6FDA, **4e**) and 4,4′-oxydiphthalic anhydride (ODPA, **4f**) were recrystallized from acetic anhydride and dried in vacuum at 160 °C for 10 h prior to use. DMAc and *N,N*-dimethylformamide (DMF) were purified by distillation under reduced pressure over calcium hydride and were stored over 4-Å molecular sieves. Xylene was refluxed with sodium and distilled under reduced pressure prior to use. Reagent-grade potassium carbonate was dried in vacuo at 130 °C for 12 h before use. The other reagents and solvents were obtained from various commercial sources and used without further purification.

Measurements

^{1}H (400 MHz) and ^{13}C (100 MHz) NMR spectra were recorded on Bruker Avance 400 MHz spectrometer using dimethyl sulfoxide-d_6 (DMSO-d_6) as the solvent and with tetramethylsilane as internal standard. The FTIR spectra were determined on a PerkinElmer SP One FTIR spectrophotometer. The glass-transition temperatures (T_g's) were measured on a PerkinElmer DSC-7 instrument at a heating rate of 20 °C/min under nitrogen protection. The second scan was immediately initiated after the sample was cooled to room temperature. The T_g values were reported from the second scan after the first heating and quenching and taken from the midpoint of the change in the slope of the baseline. The thermal stability of the polymers from 50 to 800 °C was determined with a PerkinElmer Pyris 1 TGA thermogravimetric analyzer at a heating rate of 10 °C/min under a protective nitrogen atmosphere

(120 mL/min). Microanalyses were performed with a EuroVector EA3000 Elemental Analyzer. Mass spectra (EI, 70 eV) were recorded on a HP5989B mass spectrometer. The wide-angle X-ray diffraction (WAXD) patterns were taken from 5 to 80° (2θ value) at room temperature (ca.25 °C) on polymer film with a Rigaku Geiger Flex D-Max III X-ray diffractometer, using Ni-filtered CuK_{α} radiation (operating at 40 kV and 15 mA); the scanning rate was 2°/min. The inherent viscosities of PAAs and PIs were measured at 0.5 g/dL concentration with an Ubbelohde viscometer at 30 ± 0.1 °C. Molecular weights were determined by a gel permeation chromatography (GPC) with polystyrene calibration using a Waters 510 high-performance liquid chromatography equipped with 5-μm phenogel columns (linear, 3×500 Å) arranged in series and a UV detector at 254 nm using tetrahydrofuran as eluent. The mechanical properties of the polymer films were measured on an Instron 1122 testing instrument with a 5-kg load cell at a crosshead speed of 5 mm/min on strips (0.5 cm wide, 6 cm long and ca. 0.05 mm thick), and an average of at least four replicas was used. Ultraviolet–visible (UV–Vis) spectra of the polymer films were recorded on a Shimadzu UV-1601 UV–Vis spectrophotometer. The dielectric constants were determined by the parallel plate capacitor method using a dielectric analyzer (TA instruments DEA 2970) on thin films at several frequencies in the range of 1–100 kHz. Gold electrodes were vacuum-deposited on both surfaces of dried films, followed by measuring at 25 °C in a sealed chamber maintained in nitrogen.

Synthesis of intermediates and monomer

10,10-Bis(4-hydroxyphenyl)-9(10*H*)-anthrone (1) In a 100-mL round-bottom flask, 9(10*H*)-anthrone (19.4 g, 100 mmol) was refluxed in sulfoxide chloride (60 mL) for 6 h. After removing the excess of sulfoxide chloride under vacuum, phenol (23.5 g, 0.25 mol) and xylene (60 mL) were added. The reaction mixture was stirred at 115 °C for 10 h. After reaction, the mixture was cooled to room temperature, and the crude product was obtained by filtration and washed with dichloromethane three times. After recrystallization from acetone, a gray solid compound **1** was obtained (32.0 g, 85%); mp = 306–307 °C (determined by DSC). ^{1}H NMR (400 MHz, DMSO-d_6): $\delta = 9.44$ (s, 2 H), 8.11 (d, $J = 9.6$ Hz, 2 H), 7.59 (t, $J = 7.0$ Hz, 2 H), 7.47 (t, $J = 6.8$ Hz, 2 H), 7.16 (d, $J = 7.8$ Hz, 2 H), 6.72 (d, $J = 8.8$ Hz, 4 H), 6.65 (d, $J = 8.8$ Hz, 4 H). Elem. Anal. Calcd. for $C_{26}H_{18}O_3$: C 82.52%, H 4.79%, found C 82.43%, H 4.90%. FTIR (KBr): $\nu_{max} = 3065$, 3034, 1665 (C=O stretching), 1600, 1505, 1445, 1235, 1175, 870, 760 cm^{-1}.

10,10-Bis[4-(4-nitro-3-trifluoromethylphenoxy)phenyl]-9(*10H*)-anthrone (2) In a 250-mL three-necked flask equipped with a nitrogen inlet, compound **1** (18.92 g, 50 mmol), 2-chloro-5-nitrotrifluoromethylbenzene (22.55 g, 100 mmol) and potassium carbonate (13.8 g, 100 mmol) in DMF (100 mL) were agitated at 110 °C for 8 h. Then, it was poured into 300 mL of ethanol/water (1:1) to give yellow precipitates. The crude product was obtained by filtration, washed thoroughly with water and dried in vacuum overnight. After recrystallization from DMF/ethanol, a light-yellow needle crystal compound **2** was obtained (31.77 g, 84%); mp = 214–215 °C

(determined by DSC). ^{1}H NMR (400 MHz, DMSO-d_6): δ = 8.50 (d, J = 2.8 Hz, 2 H), 8.46 (dd, J = 9.2, 2.8 Hz, 2 H), 8.21 (dd, J = 7.6, 1.2 Hz, 2 H), 7.71 (t, J = 7.2 Hz, 2 H), 7.59 (t, J = 8.0 Hz, 2 H), 7.31 (d, J = 8.0 Hz, 2 H), 7.23–7.20 (m, 6 H), 7.14 (d, J = 9.2 Hz, 4 H). ^{13}C NMR (100 MHz, DMSO-d_6): δ = 183.8, 160.2, 153.1, 148.9, 144.1, 142.4, 134.2, 132.3, 131.8, 131.1, 130.6, 128.4, 127.4, 124.1 (q, $^{3}J_{C–F}$ = 5 Hz), 123.8 (q, $^{1}J_{C–F}$ = 271 Hz), 120.6, 120.4 (q, $^{2}J_{C–F}$ = 34 Hz), 119.0, 57.3. Elem. Anal. Calcd. for $C_{40}H_{22}F_6N_2O_7$: C 63.50%, H 2.93%, N 3.70%, found C 63.41%, H 3.08%, N 3.62%. FTIR (KBr): ν_{max} = 3092, 3067, 1667 (Ar–CO–Ar stretching), 1626, 1594, 1486, 1531 and 1350 (–NO_2 stretching), and 1332 (C–N stretching), 1268 (Ar–O–Ar stretching), 1165 (C–F stretching), 1120, 1050 and 1018 (Ar–O–Ar stretching), 903, 832, 794 cm^{-1}.

10,10-Bis[4-(4-amino-3-trifluoromethylphenoxy)phenyl]-9(*10H*)-anthrone (3, BATFPA) To a 250-mL three-necked flask equipped with a dropping funnel and a reflux condenser, dinitro compound **2** (7.56 g, 10 mmol), palladium on activated carbon (10% Pd/C) (0.2 g) and anhydrous ethanol (100 mL) were added, and after heating to refluxing temperature with stirring, hydrazine monohydrate (10 mL) was added dropwise in 2 h. After addition of hydrazine monohydrate, the mixture was refluxed for additional 8 h. Then, the mixture was filtered and the resultant solid was extracted using enough ethanol. On concentrating all the ethanol solution, yellow precipitation appeared, which was filtered and recrystallized from ethanol to give a needle crystal diamine compound **3** (6.13 g, 88%); mp = 196–197 °C (determined by DSC). ^{1}H NMR (400 MHz, DMSO-d_6): δ = 8.17 (d, J = 7.6, 2 H), 7.64 (t, J = 8.2 Hz, 2 H), 7.52 (t, J = 7.6 Hz, 2 H), 7.20 (d, J = 7.6, 2 H), 6.93–6.88 (m, 8 H), 6.82–6.79 (m, 4 H), 5.45 (s, 4 H, NH_2). ^{13}C NMR (100 MHz, DMSO-d_6): δ = 183.9, 157.5, 149.6, 146.4, 142.4, 140.5, 133.9, 131.6, 131.4, 130.0, 128.0, 127.2, 125.3 (q, $^{1}J_{C–F}$ = 271 Hz), 123.7, 121.9 (q, $^{2}J_{C–F}$ = 30 Hz), 121.0, 119.0, 111.1, 56.9. Elem. Anal. Calcd. for $C_{40}H_{26}F_6N_2O_3$: C 68.96%, H 3.76%, N 4.02%; found C 68.88%, H 3.88%, N 3.95%. FTIR (KBr): ν_{max} = 3464, 3380 (N–H stretching), 3066, 1672 (Ar–CO–Ar stretching), 1600, 1492, 1338 (C–N stretching), 1243 (Ar–O–Ar stretching), 1159 (C–F stretching), 1125, 1050 (Ar–O–Ar stretching), 935, 858, 826, 756 cm^{-1}.

Preparation of polymer films

The new PIs were synthesized through a conventional two-step procedure via the polycondensation of equal molar amounts of diamine **3** with several aromatic dianhydrides to form poly(amic acid) (PAA) precursors, followed by thermal cyclodehydration. A typical preparation procedure of the PI-**6b** was described as follows: In a 50-mL three-necked round bottle flask equipped with a mechanical stirrer, the diamine **3** (1.6878 g, 3.0 mmol) was dissolved in DMAc (7.0 g) under a nitrogen purge. The flask was submerged in ice bath, and BPDA (**4b**) (0.8827 g, 3.0 mmol) powder was added in one portion. Extra 6.0 g DMAc was then added to adjust the solid content 15 wt%. The mixture was stirred in ice bath for 1 h and then stirred at ambient temperature overnight (ca.12 h) to obtain a viscous PAA-**5b**, whose inherent viscosity in DMAc was 1.18 dL/g, measured at a concentration of 0.5 g/

dL at 30 °C. The corresponding polymer film was prepared by thermal imidization of its solution cast onto flat and clean glass plates, which was dried in an vacuum oven at 80 °C for 10 h and then cured by a stepped thermal sequence (150 °C/1 h, 250 °C/1 h, 280 °C/1 h). The PI-**6b** thin film was stripped off from the glass plate when it was cooled. FTIR (film): $\nu_{max} = 1776$ (asymmetric C=O stretch), 1720 (symmetric imide C=O stretch), 1663 (C=O stretch of anthrone units) 1600–1500 (aromatic C=C stretch), 1380 (C–N stretch), 1240 (Ar–O–Ar stretch), 1085, 1024, 720 cm^{-1} (imide ring deformation).

The other corresponding PIs were synthesized by the similar method described above.

Results and discussion

Synthesis of monomer

As outlined in Scheme 1, the diamine monomer, 9,9-bis[4-(4-amino-3-trifluoromethylphenoxy)phenyl]-9(*10H*)-anthrone (**3**, **BATFPA**) was obtained through a three-step procedure. Although biphenol intermediates of the cardo type can be obtained by condensation of ketones with phenols in the presence of Friedel–Crafts catalysts or mineral acids and others [26], the yield of this method is often not high. However, 10,10-bis(4-hydroxyphenyl)-9(*10H*)-anthrone (**1**) can be prepared in 85% yield via one-pot, two-step synthetic procedure by reaction of 9(*10H*)-anthrone with thionyl chloride, affording intermediate 10,10-dichloro-9(*10H*)-anthrone, followed by treatment with phenol in refluxing xylene without isolation of the intermediate, according to the reported similar method [33]. Then, the nucleophilic substitution reaction of bisphenol intermediate **1** with 2-chloro-5-nitrotrifluoromethylbenzene in the presence of potassium carbonate gave the dinitro compound, 9,9-bis[4-(4-nitro-3-trifluoromethylphenoxy)phenyl]-9(*10H*)-anthrone (**2**).

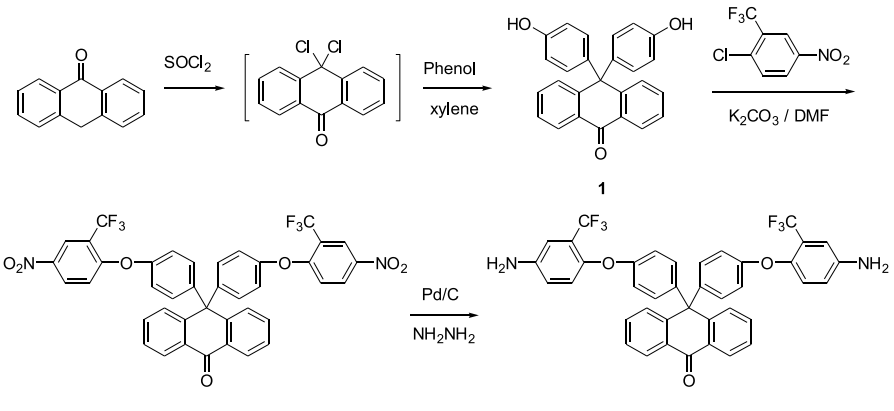

Scheme 1 The synthetic route to the target diamine **3**

Finally, the novel diamine **3** was obtained by catalytic hydrogenation of the dinitro **2** using hydrazine monohydrate and a catalytic amount of palladium on activated carbon in refluxing ethanol. The structures of these compounds were confirmed by elemental analysis, FTIR and NMR spectroscopy. As indicated in "Experimental" section, the elemental analysis data of the dinitro and diamine compounds were found to correspond well with the calculated values for their structures. Besides, the FTIR spectrum of the dinitro **2** gave two characteristic bands at 1531 and 1350 cm^{-1} ($–NO_2$ asymmetric and symmetric stretching), while the characteristic absorptions of the nitro group disappeared and the amino group showed a pair of N–H stretching absorptions in the region of 3300–3500 cm^{-1} in the FTIR spectrum of the diamine **3**. The ^{1}H NMR and ^{13}C NMR spectra of the dinitro **2** in DMSO-d_6 solution are depicted in Fig. 1. In the ^{1}H NMR spectrum (Fig. 1a), almost all aromatic protons except for H^g and H^e were clearly distinguished.

Figure 2 presents the ^{1}H NMR and ^{13}C NMR spectra of the diamine **3** in DMSO-d_6 solution. In its ^{1}H NMR spectrum (Fig. 2a), the signals in the range of 8.17–6.79 ppm were ascribed to the protons of the aromatic ring and the signal in 5.45 ppm was ascribed to the protons of the primary aromatic amine group. The ^{13}C NMR spectrum (Fig. 2b) showed signals, resonating in the region of 183.9–56.9 ppm. A clear quartet centered at 121.9 ppm due to the CF_3-attached carbon C^{18} with the constant about 30 Hz by two-bond C–F coupling and the C^{19} showed quartet signals at about 125.3 ppm with the coupling constant ($^1J_{C–F}$ = 271 Hz).

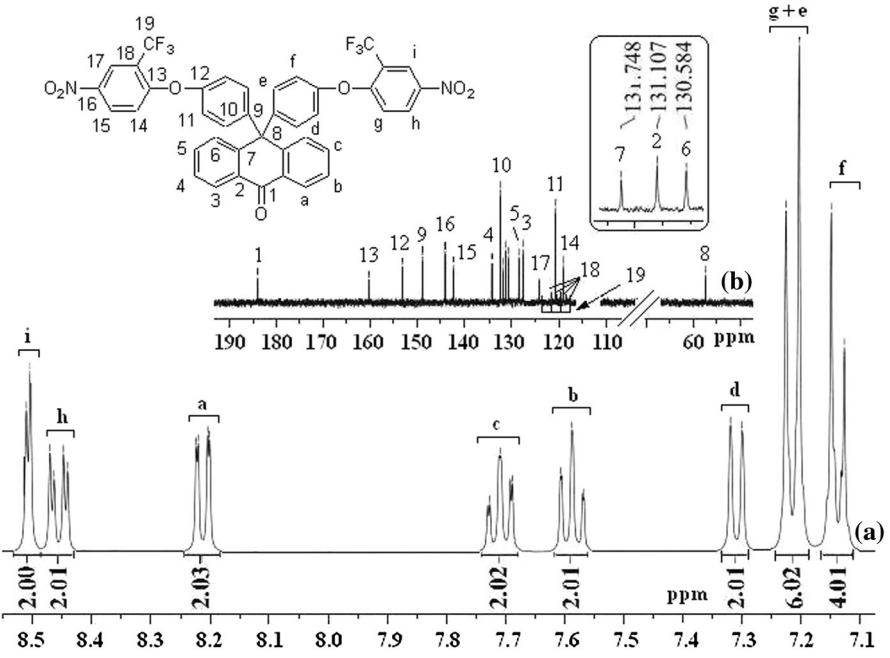

Fig. 1 ^{1}H NMR (**a**) and ^{13}C NMR (**b**) of the dinitro **2**

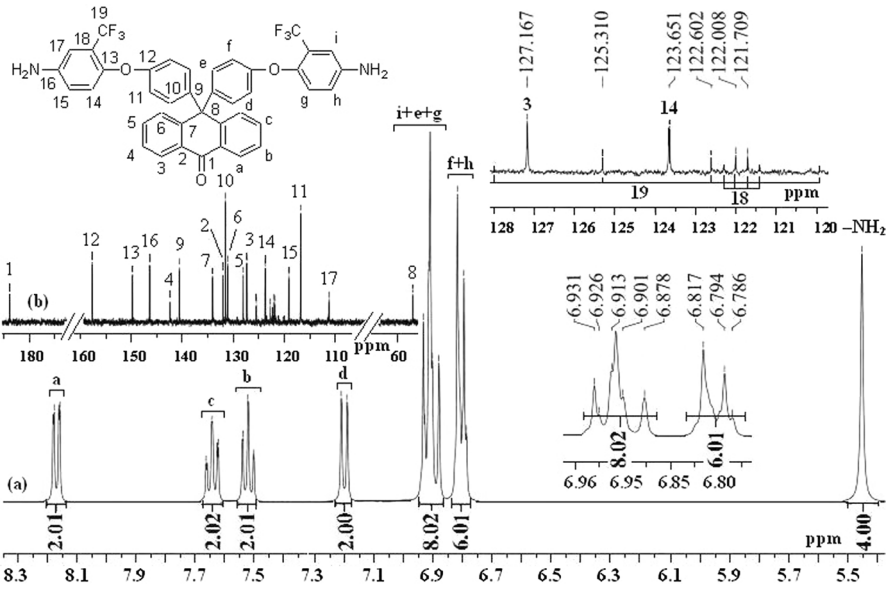

Fig. 2 ^{1}H NMR (**a**) and ^{13}C NMR (**b**) spectra of the diamine **3**

Polymer synthesis

As shown in Scheme 2, a series of new cardo fluorinated PIs containing anthrone units (**6a**–**6f**) were synthesized via the conventional two-step polymerization procedure from the diamine **3** with commercially available aromatic dianhydrides **4a**–**4f** (PMDA, BPDA, HQDPA, BTDA, 6FDA and ODPA), involving ring-opening polyaddition forming poly(amic acid) (PAA) precursors (**5a**–**5f**) and subsequent thermal imidization. In all cases, the polymerization was performed effectively at ambient temperature for 10–12 h to afford viscous PAA solution by reacting equimolar amounts of **3** with **4** at a concentration of 15% solids in dry DMAc. The polymerization results and the corresponding data are summarized in Table 1. As shown in Table 1, the inherent viscosity (η_{inh}) of the PAA solution measured in DMAc in 0.5 g/dL concentration at 30 °C was in the range of 0.82–1.18 dL/g. Tough and flexible PI films were then achieved in high yields (94–98%) by casting the PAA solution on the glass plate followed by thermally curing process at 280 °C in a tube furnace under a flow of nitrogen atmosphere. The inherent viscosity of PIs ranged from 0.76 to 1.12 dL/g in DMF, indicating that these polymers with relatively high molecular weights to cast flexible and tough films. Furthermore, the PI-**6e** shows the weight-average and number-average molecular weights of 48,500 g/mol and 26,800 g/mol, respectively, with the polydispersity index (M_w/M_n) value of 1.81, as determined by gel permeation chromatography (GPC) compared to the polystyrene standard using THF as the eluent.

The formation of the resulting fluorinated PIs containing anthrone groups was confirmed by FTIR and elemental analysis. The typical FTIR spectra of PAA-**5b**

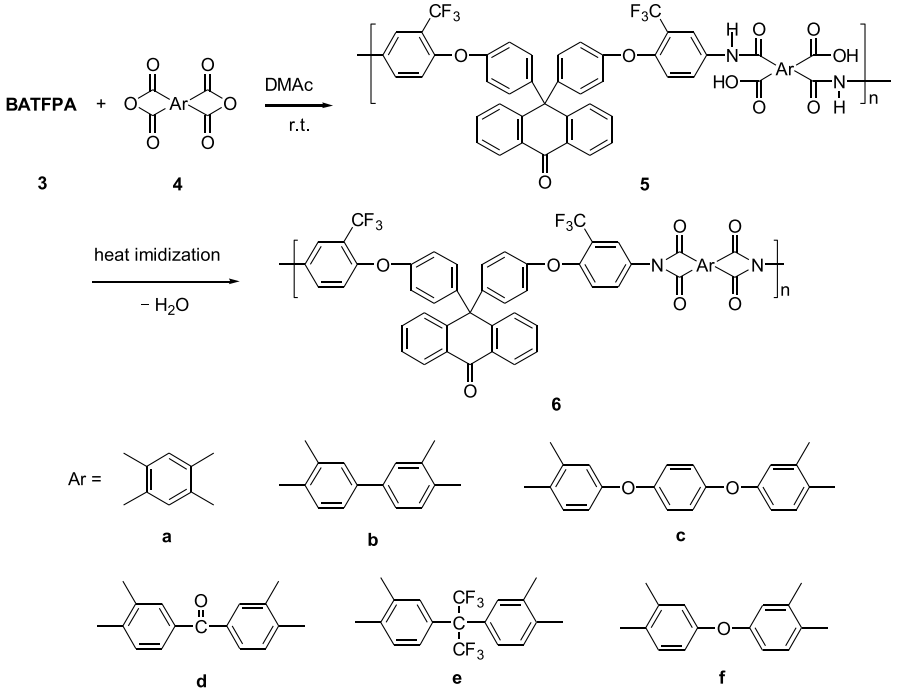

Scheme 2 Preparation of the new cardo PIs (**6a–6f**)

Table 1 Inherent viscosities of the PAAs, PIs and their elemental analysis data

PAAs		PIs			Elemental analysis (%) of PIs[c]			
Code	η_{inh} (dL/g)[a]	Code	η_{inh} (dL/g)[b]	Yield (%)	Formula (molecular weight)	C	H	N
5a	0.85	**6a**	0.90	98	$(C_{50}H_{24}F_6N_2O_7)_n$ $(878.74)_n$	68.22 (68.34)	2.94 (2.75)	3.11 (3.19)
5b	1.18	**6b**	1.12	97	$(C_{56}H_{28}F_6N_2O_7)_n$ $(954.84)_n$	70.28 (70.44)	3.11 (2.96)	2.77 (2.93)
5c	0.94	**6c**	0.80	94	$(C_{62}H_{32}F_6N_2O_9)_n$ $(1062.93)_n$	69.85 (70.06)	3.17 (3.03)	2.38 (2.64)
5d	1.08	**6d**	0.98	97	$(C_{57}H_{28}F_6N_2O_8)_n$ $(982.85)_n$	69.78 (69.66)	2.98 (2.87)	2.72 (2.85)
5e	0.82	**6e**	0.76	96	$(C_{59}H_{28}F_{12}N_2O_7)_n$ $(1104.86)_n$	64.03 (64.14)	2.68 (2.55)	5.33 (2.54)
5f	1.06	**6f**	0.93	95	$(C_{56}H_{28}F_6N_2O_8)_n$ $(970.83)_n$	69.12 (69.28)	3.02 (2.91)	2.79 (2.89)

[a]Measured at a concentration of 0.5 g/dL in DMAc at 30 °C

[b]Measured at a concentration of 0.5 g/dL in DMAc at 30 °C

[c]Theoretical percentages are in parentheses

film and the corresponding fully cyclized PI-**6b** film are shown in Fig. 3. As displayed in Fig. 3b, the FTIR spectrum of PI-**6b** exhibited the characteristic imide moiety absorption at around 1380 cm^{-1} due to stretching vibration of the C–N bond that was newly formed in the polymer backbones. The other characteristic peaks observed at around 1776, 1720 and 720 cm^{-1} were assigned to carbonyl asymmetric and symmetric stretching vibration, and flexural vibration of imide ring, respectively. Besides, the characteristic absorption at 1663 cm^{-1} due to the carbonyl stretching of anthrone units was also observed. The PAA **5b** vibration (Fig. 3a) included three stronger bands for carbonyl stretch of the carboxylic acid at 1719 cm^{-1}, N–H stretch of amide II mode at 1535 cm^{-1} and carbonyl stretch of anthrone units at 1664 cm^{-1}. As mentioned above, the complete imidization of PAA was easily identified by the disappearance of the amide-related bands and the appearance of the corresponding imide bands after thermal imidization. Additionally, the results of the elemental analyses of all the thermally cured PIs are listed in Table 1, in which the values found were in good agreement with the calculated ones of the proposed structures.

Thermal properties

Differential scanning calorimetry (DSC) and thermogravimetric analysis (TGA) were used to evaluate the thermal properties of the PIs (**6a**–**6f**), and the corresponding data are summarized in Table 2. No crystallization or melting peaks were observed in the DSC curves (Fig. 4), which also revealed the amorphous structure of these polymers and agreed well with the WAXD results. The glass-transition temperatures (T_g's) of the present PIs were in the range of 259–329 °C. The high T_g

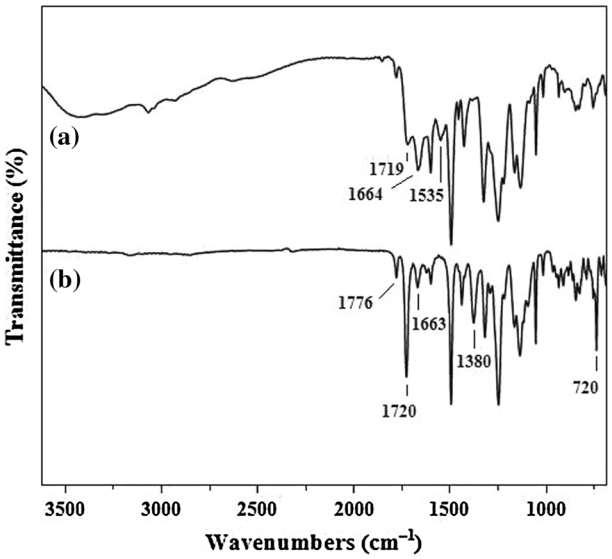

Fig. 3 FTIR spectra of the PAA-**5b** (**a**) and PI-**6b** (**b**)

Table 2 Thermal properties of the PIs (**6a**–**6f**)

PIs	T_g (°C)[a]	T_{d5} (°C)[b]	T_{d10} (°C)[c]	T_{max} (°C)[d]	R_w (%)[e]
PI-**6a**	329	526	545	551	59
PI-**6b**	306	522	548	562	62
PI-**6c**	259	530	556	541	62
PI-**6d**	300	525	550	546	64
PI-**6e**	289	521	542	561	59
PI-**6f**	274	516	543	538	57

[a]Midpoint temperature of the baseline shift on the second DSC heating trace

[b]Temperature at 5% weight loss under nitrogen

[c]Temperature at 10% weight loss under nitrogen

[d]Temperature at the maximum-rate degradation under nitrogen atmosphere

[e]Residual weight percentage at 800 °C under nitrogen

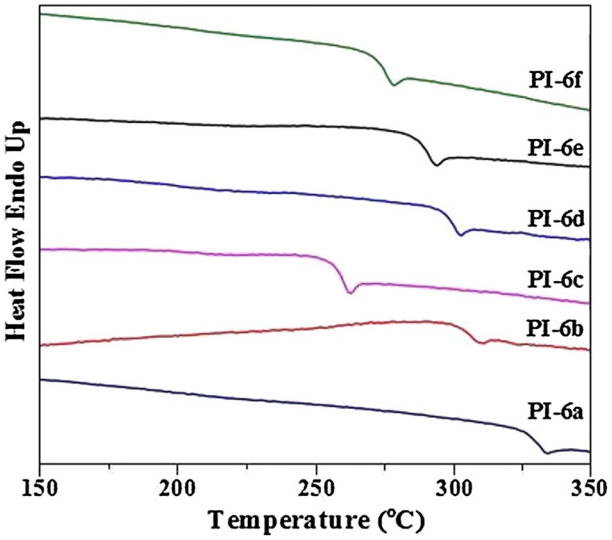

Fig. 4 DSC curves of the PIs (**6a**–**6f**)

values mainly originated from the inherent rigidity of the polymer backbones, which indicated the introduction of bulky anthrone pendent group into the polymer main chains could improve their T_g's significantly. Meanwhile, depending on the structure of aromatic dianhydride, the T_g values tended to display the increasing order of HQDPA < ODPA < 6FDA < BTDA < BPDA < PMDA. This order was perfectly matched with the rigidity of the polymer backbones. It was observed that PI-**6a** exhibited the highest T_g (329 °C), which may be due to the synergistic effect of bulky cardo moieties [26], trifluoromethyl groups [4] and the rigid PMDA (**4a**) [5]. Among the PIs tested, PI-**6c** obtained from HQDPA (**4c**) gave the lowest T_g (259 °C)

because of the presence of more flexible ether linkages in dianhydride units. Moreover, the T_g values of these polymers are higher than those of commercial poly(ether imide), Ultem 1000 (T_g = 217 °C) based on BPADA [bisphenol-A (diphthalic anhydride)] and MPD (*m*-phenylene diamine) [34] and also comparable to BTDA–ODA (T_g = 279 °C)-based polyimides except for PI-**6c** and PI-**6e** [1]. However, the T_g values of these polymers are lower than that of Kapton film derived from PMDA–ODA (T_g = 390 °C) [35].

The thermal stability data of these PIs based on the thermo gravimetric analysis (TGA) and differential thermal gravity (DTG) in nitrogen atmosphere are also presented in Table 2. The maximum weight loss temperature (T_{max}) ranged from 538 to 562 °C, and the 5% weight loss temperatures at (T_{d5}) and the residual weights at 800 °C were in the range of 521–530 °C and 57–64%, respectively, implying that all the PIs possess excellent thermal stability. Typical TGA and DTG curves of the PI-6b are depicted in Fig. 5. As observed, the introduction of flexible ether linkages, along with bulky anthrone pendent units and trifluoromethyl groups, into the polymer backbone can still endow the polymers good thermal stability. The fairly high thermal stability, combined with the high T_g values for the resulting PIs, shows that some of them are able to withstand elevated processing temperatures and have potential application in microelectronic manufacturing, the packaging industry and so on.

Solubility

The solubilities of the PI samples (**6a**–**6f**) were tested qualitatively in various solvents, and the results are listed in Table 3. It can be seen that the obtained PIs exhibited good solubility in dipolar solvents such as NMP, DMF and DMAc at room temperature, which might be attributed to the introduction of bulky

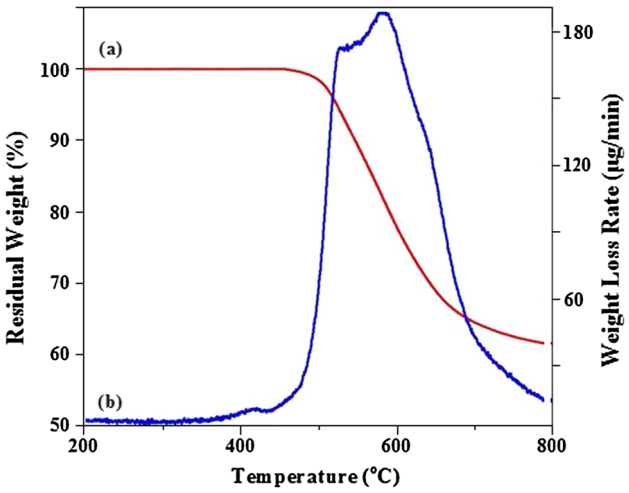

Fig. 5 TGA (**a**) and DTG (**b**) curves of the PI-**6b**

Table 3 Solubility in various solvents of the PIs (**6a**–**6f**)[a]

Solvent	PI-**6a**	PI-**6b**	PI-**6c**	PI-**6d**	PI-**6e**	PI-**6f**
NMP	+ +	+ +	+ +	+ +	+ +	+ +
DMF	+ +	+ +	+ +	+ +	+ +	+ +
DMAc	+ +	+ +	+ +	+ +	+ +	+ +
DMSO	+ –	+ –	+ –	+ –	+ –	+ –
m-Cresol	– –	– –	+ –	– –	+ –	+ –
THF	+ –	+ –	+ –	+ –	+ +	+ –
$CHCl_3$	– –	– –	– –	– –	+ –	– –
Acetone	– –	– –	– –	– –	– –	– –
Toluene	– –	– –	– –	– –	– –	– –

[a]Measured by dissolving 10 mg polymer sample in 1 mL solvent at room temperature. ++ soluble; +– swelled slightly or partially soluble; – – insoluble; *NMP* *N*-methyl-2-pyrrolidone; *DMAc* *N,N*-dimethylacetamide; *DMF* *N,N*-dimethylformamide; *DMSO* dimethylsulfoxide; *THF* tetrahydrofuran

trifluoromethyl and anthrone pendent groups, as well as flexible ether linkages, inhibiting close packing and reducing the interchain interactions to enhance solubility. However, the solubilities of these PIs in DMSO were inferior. Besides, their solubilities were also affected by the structure of the used dianhydride monomers. For example, PI-**6e** was even soluble in THF at room temperature because of the presence of hexafluoroisopropylidene units in its main chain. On the other hand, the present test results of the PI-**6c** and PI-**6f** seemed to show the incorporation of more flexible ether linkages into macromolecular backbones had little influence on their solubilities in this series.

Crystallinity and tensile properties

The crystallinity of all PI samples (**6a**–**6f**) was examined by wide-angle X-ray diffraction (WAXD) analysis, as shown in Fig. 6. As expected, all the polymers failed to show any crystallinity. Clearly, it can be ascribed to the presence of the flexible ether linkages, bulky anthrone cardo units and trifluoromethyl groups, which reduced the intra- and inter-polymer chain interactions, resulting in loose polymer chain packaging and aggregates. Therefore, the amorphous nature of the resulting PIs would endow them a good solubility.

The PIs films (**6a**–**6f**), prepared by casting the PAA solution on the glass plate followed by the thermal curing in the following procedure 80 °C for 10 h, 150 °C, 250 °C and 280 °C for 1 h at each temperature, were lightly colored, optically transparent, flexible and tough. These films were subjected to mechanical property tests (Fig. 7), and the corresponding results are summarized in Table 4. The prepared PI films exhibited tensile strength, tensile modulus and elongation at break in the range of 63.5–101.7 MPa, 1.94–2.85 GPa and 3.7–13.6%, respectively, indicating that they could be considered as hard and strong materials.

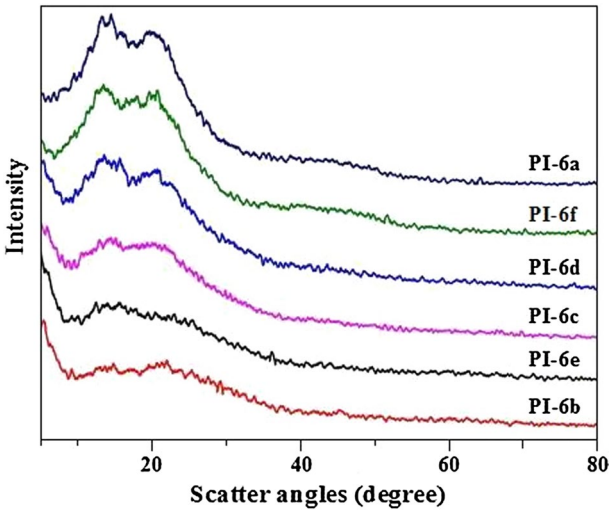

Fig. 6 WAXD curves of the PIs (**6a–6f**)

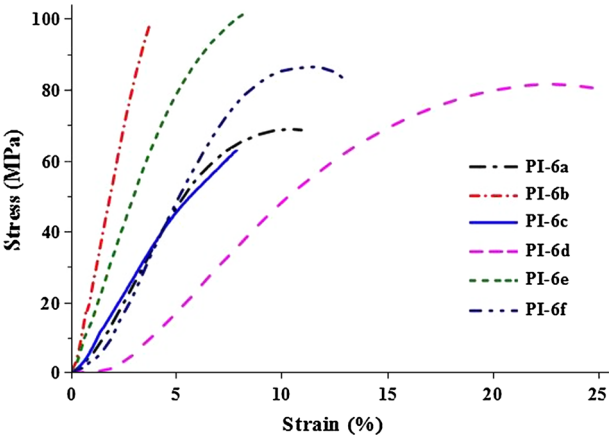

Fig. 7 Stress–strain plots of the PIs (**6a–6f**)

Table 4 Mechanical properties of the PIs (**6a–6f**)

PIs	Tensile strength (MPa)	Elongation at break (%)	Tensile modulus (GPa)
6a	68.6	10.9	2.08
6b	98.3	3.7	2.85
6c	63.5	8.1	1.94
6d	81.9	13.6	2.16
6e	101.7	8.3	2.42
6f	86.2	13	2.25

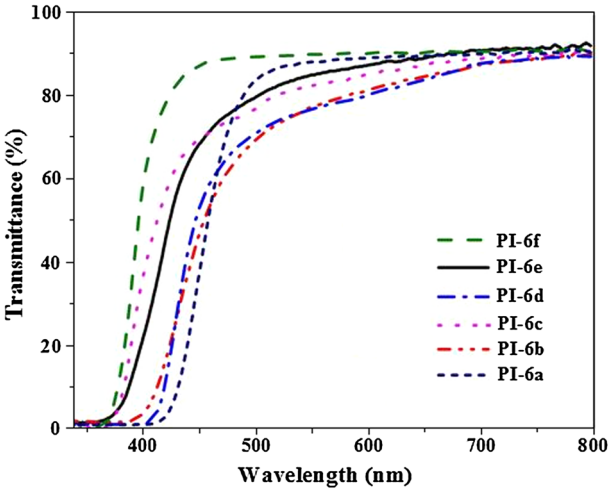

Fig. 8 UV–Vis spectra of the PIs (**6a**–**6f**)

Table 5 Optical transparency, dielectric constant and water uptake of the PIs (**6a**–**6f**)

PIs	Film thickness (μm)	Water uptake (%)	λ_0 (nm)[a]	Transparency (%)[b]	Transparency (%)[c]	Dielectric constant[d]	
						1 kHz	1 MHz
6a	54	0.55	408	89.0	89.5	2.75	2.67
6b	51	0.48	378	81.2	87.2	2.70	2.62
6c	53	0.83	363	85.1	88.8	2.56	2.48
6d	50	0.68	402	80.2	87.4	3.05	2.96
6e	48	0.36	336	87.3	90.7	2.49	2.35
6f	49	0.72	360	90.1	90.7	2.51	2.45
PI[e]	51	1.05	444	77.2	86.2	3.55	3.42

[a]Cutoff wavelength

[b]Transparency at 600 nm

[c]Transparency at 700 nm

[d]Dry dielectric constant at 25 °C

[e]Prepared from PMDA and 4,4′-oxydianiline (ODA) in our laboratory using the similar method

Optical transparency

Figure 8 shows the UV–Vis spectra of the PI films (**6a**–**6f**) evaluated by UV–Vis measurements with approximately 50 μm thickness, and some data are also reported in Table 5. As shown in Table 5, the cutoff wavelength (λ_0) values of the obtained PI films ranged from 336 to 408 nm, and the optical transmittance values at the wavelength of 600 nm were all higher than 80%, which revealed that all polymers were near colorless and had high transmittances. Obviously, the good optical transparency

observed is attributed not only to the bulkiness of the cardo anthrone pendent groups [26], but also to the strong electron-withdrawing trifluoromethyl groups, decreasing effectively the inter- and intramolecular CTC between polymer chains as a result of steric hindrance and the inductive effect [4]. In addition, the PI-**5e** derived from 6FDA showed the shortest λ_0 value, together with higher optical transparency in contrast to the other analogs in this series because the 6FDA with the hexafluoroisopropyl groups can further reduce CTC formation.

Dielectric constants and water absorption

The dielectric constants at selective frequencies and water uptake of all PIs (**6a**–**6f**) are also listed in Table 5. For example, these PIs revealed dielectric constants at 1 MHz in the range of 2.35–2.96. Obviously, the low dielectric constant values of these polymers were mainly associated with the fact that trifluoromethyl possessed large free volume, strong electronegativity and low polarizability, which was contributed to less efficient molecular chain packing and increased interchain free volume [36]. Additionally, the existence of the bulky anthrone fragments in the backbone of polymers hindered the compact stacking of molecules, decreasing the dielectric constants to a certain extent [26]. Furthermore, the dielectric constant values of these films are lower than those of Kapton H ($\varepsilon = 3.5$ at 1 kHz), Upilex R ($\varepsilon = 3.5$ at 1 kHz), Upilex S ($\varepsilon = 3.5$ at 1 kHz) and Ultem 1000 ($\varepsilon = 3.15$ at 1 kHz) types of polyimide materials and comparable to those of many semifluorinated poly(ether imide)s (e.g., 6FDA–MPD: $\varepsilon = 3{:}0$) [1].

Table 5 also presents the small water uptakes of the prepared PIs (**6a**–**6f**) in the range of 0.36–0.83%, which is probably attributed to the water proofing effect of the fluorine atoms [36]. The low water absorption ensured these polymers had stable dielectric constants. In comparison, as seen from Table 5, all PIs exhibited lower water uptake than the PI film derived from PMDA–ODA. It should be noted that the PI-**6e** exhibited the lowest water absorption (0.36%) in comparison with those of the other PIs in this series due to its highest fluorine content in the repeat unit.

Conclusions

A new aromatic diamine containing ether, trifluoromethyl and anthrone groups, 10,10-bis[4-(4-amino-2-trifluoromethylphenoxy)phenyl]-9(*10H*)-anthrone was successfully synthesized and reacted with various aromatic dianhydrides to yield a series of novel cardo fluorinated polyimides (PIs) containing anthrone pendent groups by two-step polycondensation method. Owing to the presence of trifluoromethyl and aryl ether groups into the polymer backbone, along with the cardo anthrone structure of the repeat unit, the obtained PIs exhibited good solubility in organic solvents and could be solution-cast into transparent and strong films. They also showed excellent thermal stability, high optical transparency and low dielectric constant. As a result, these new PIs may be considered as promising processable high-temperature materials for applications in microelectronic and optical devices.

Acknowledgements The financial support for this work provided by the National Natural Science Foundation of China (Nos. 21564005, 51663011, 21965014), the Research Program of Jiangxi Science and Technology Department (No. 20192BBE50049), the Ground Project for Science and Technology of Jiangxi Universities (No. KJLD14022) and the Research Program of Jiangxi Province Department of Education (No. GJJ14236) is gratefully acknowledged.

References

1. Maier G (2001) Low dielectric constant polymers for microelectronics. Prog Polym Sci 26:3–65
2. Choi M-C, Kim Y, Ha C-S (2008) Polymers for flexible displays: from material selection to device applications. Prog Polym Sci 33:581–630
3. Ji D, Li YT, Zou Y, Chu M, Zhou K, Liu JY, Tian GF, Zhang ZY, Zhang X, Li LQ, Wu DZ, Dong HL, Miao Q, Fuchs H, Hu WP (2008) Copolymer dielectrics with balanced chain-packing density and surface polarity for high-performance flexible organic electronics. Nat Commun 9:2339–2347
4. Lewis J (2006) Material challenge for flexible organic devices. Mater Today 9:38–45
5. Sroog CE (1991) Polyimides. Prog Polym Sci 16:561–694
6. Hasegawa M, Horie K (2001) Photophysics, photochemistry, and optical properties of polyimides. Prog Polym Sci 26:259–335
7. Ding MX (2007) Isomeric polyimides. Prog Polym Sci 32:623–668
8. Liaw D-J, Wang K-L, Huang Y-C, Lee K-R, Lai J-Y, Ha C-S (2012) Advanced polyimide materials: syntheses, physical properties and applications. Prog Polym Sci 37:907–974
9. Hariharan A, Kumar S, Alagar M, Dinakaran K, Subramanian K (2018) Synthesis, photophysical and electrochemical properties of polyimides of tetraaryl imidazole. Polym Bull 75:93–107
10. Amininasab SM, Esmaili S, Taghavi M, Shami Z (2016) Fabrication and characterization of novel high-performance fluorinated polyimides with xanthene pendent architecture: study of thermal, photophysical, antibacterial and heavy metal ion adsorption behavior. J Fluor Chem 192:48–57
11. Tapaswi PK, Choi M-C, Jeong K-M, Ando S, Ha C-S (2015) Transparent aromatic polyimides derived from thiophenyl-substituted benzidines with high refractive index and small birefringence. Macromolecules 48:3462–3474
12. Rafiee Z, Khalili S (2013) Synthesis and characterization of highly soluble and thermally stable new polyimides based on 3,5-diamino benzoyl amino phenyl-14H-dibenzoxanthene. Polym Bull 70:2423–2435
13. Wen PS, He R, Li X-D, Lee M-H (2017) Syntheses and characterizations of high refractive index and low birefringence polyimides containing spirobifluorene in the side chain. Polymer 117:76–83
14. Kanosue K, Peckus D, Karpicz R, Tamulevic T (2015) Polyimide and imide compound exhibiting bright red fluorescence with very large stokes shifts via excited-state intramolecular proton transfer. Macromolecules 48:1777–1785
15. Terraza CA, Tagle LH, Santiago-García JL, Canto-Acosta RJ, Aguilar-Vega M, Hauyon RA, Coll D, Ortiz P, Perez G, Herrán L, Comesaña-Gándara B, McKeown NB, Tundidor-Camba A (2018) Synthesis and properties of new aromatic polyimides containing spirocyclic structures. Polymer 137:283–292
16. Hu XF, Yan JL, Wang YX, Mu HL, Wang ZK, Cheng HY, Zhao FY, Wang Z (2017) Colorless polyimides derived from *2R,5R,7S,10S*-naphthanetetracarboxylic dianhydride. Polym Chem 8:6165–6172
17. Liu YW, Zhang Y, Lan Q, Qin ZX, Liu SW, Zhao CY, Chi ZG, Xu JR (2013) Synthesis and properties of high-performance functional polyimides containing rigid nonplanar conjugated tetraphenylethylene moieties. J Polym Sci Part A Polym Chem 51:1302–1314
18. Zhao J, Peng L, Zhu Y-L, Zheng AM, Shen Y-Z (2016) Tristable data storage device of soluble polyimides based on novel asymmetrical diamines containing carbazole. Polym Chem 7:1765–1772
19. Iqbal A, Lee SH, Park OO, Siddiqi HM, Akhter T (2016) Synthesis and characterization of blue light emitting redox-active polyimides bearing noncoplanar fused carbazole-triphenylamine. New J Chem 40:5285–5293
20. Dhara MG, Banerjee S (2010) Fluorinated high-performance polymers: poly(arylene ether)s and aromatic polyimides containing trifluoromethyl groups. Prog Polym Sci 35:1022–1077

21. Sheng S-R, Li D-P, Liu X-L, Lai T-Q, Song C-S (2011) Organosoluble, low dielectric constant fluorinated polyimides based on 9,9-bis[4-(4-amino-2-trifluoromethylphenoxy)phenyl]xanthene. Polym Int 60:1185–1193
22. Yeo H, Goh M, Ku BC, You NH (2015) Synthesis and characterization of highly-fluorinated colorless polyimides derived from 4,4′-((perfluoro-[1,10-biphenyl]-4,4′-diyl)bis(oxy))bis(2,6-dimethylaniline) and aromatic dianhydrides. Polymer 76:280–286
23. Vaganova TA, Plekhanov AI, Simanchuk AE, Mikerin SL, Spesivtsev EV, Karpova EV, Frolova TS, Malykhin EV (2017) Synthesis and characterization of novel polyhalogenaromatic polyimide material for electro-optic applications. J Fluor Chem 19:70–78
24. Mi ZM, Liu ZX, Tian CS, Zhao XG, Zhou HW, Wang DM, Chen CH (2017) Soluble polyimides containing 1,4:3,6-dianhydro-d-glucidol and fluorinated units: preparation, characterization, optical, and dielectric properties. J Polym Sci Part A Polym Chem 55:3253–3265
25. Jia MC, Zhou MT, Li YJ, Lu GL, Huang XY (2018) Construction of semi-fluorinated polyimides with perfluorocyclobutyl aryl ether-based side chains. Polym Chem 9:920–930
26. Korshak VV, Vinogradova SV, Vygodski YS (1974) Cardo polymers. J Macromol Sci Rev Macromol Chem C11:45–142
27. Liaw D-J, Liaw B-Y (1999) Synthesis and properties of new polyimides derived from 1,1-bis[4-(4-aminophenoxy)phenyl]cyclododecane. Polymer 40:3183–3189
28. Sheng S-R, Zhang W, Lu C, Wan J, Liu X-L, Song C-S (2012) Synthesis and characterization of new cardo polyimides derived from 9,9-bis[4-(4-aminophenoxy)phenyl]xanthene. J Appl Polym Sci 126:297–303
29. Liu JT, Chen GF, Mushtaq N, Fang XZ (2015) Synthesis of organosoluble and light-colored cardo polyimides via aromatic nucleophilic substitution polymerization. Polym Adv Technol 26:1519–1527
30. Yi L, Li CY, Huang W, Yan DY (2016) Soluble and transparent polyimides with high T_g from a new diamine containing *tert*-butyl and fluorene units. J Polym Sci Part A Polym Chem 54:976–984
31. Lu YH, Hao JC, Li L, Song J, Xiao GY, Zhao HB, Hu ZZ, Wang TH (2017) Preparation and gas transport properties of thermally induced rigidmembranes of copolyimide containing cardo moieties. React Funct Polym 119:134–144
32. Yang YH, Xia JC, Ding ZJ, Zheng YX, Ding SJ, Shen YZ (2018) Synthesis and resistive switching characteristics of polyimides derived from 2,7-aryl substituents tetraphenyl fluorene diamines. Eur Polym J 108:85–97
33. Guo D-D, Jiang J-W, Liu Y-J, Liu X-L, Sheng S-R (2015) New fluorinated xanthene-containing polybenzoxazoles with low dielectric constants. J Fluor Chem 175:169–175
34. Chung TS, Vora RH, Jaffe M (1991) Fluoro-containing polyimide blends: prediction and experiments. J Polym Sci Polym Chem Ed 29:1207–1212
35. Takekoshi T (1996) In: Kirk-Othmer (ed) Encyclopedia of chemical technology, vol 19. Wiley, New York
36. Hougham G, Tesoro G, Shaw J (1994) Synthesis and properties of highly fluorinated polyimides. Macromolecules 27:3642–3649